

1 Patients with mesenchymal tumours and high *Fusobacteriales* prevalence have worse prognosis 2 in colorectal cancer (CRC)

4 Manuela Salvucci¹, Nyree Crawford², Katie Stott², Susan Bullman^{3,4}, Daniel B. Longley², and
5 Jochen H.M. Prehn^{1*}

7 ¹Centre for Systems Medicine, Department of Physiology and Medical Physics, Royal College of
8 Surgeons in Ireland, Dublin, Ireland;

9 ²Patrick G. Johnston Centre for Cancer Research, School of Medicine, Dentistry and Biomedical
10 Science, Queen's University Belfast, Northern Ireland, UK;

11 ³Dana-Farber Cancer Institute, Harvard Medical School, Boston, USA;

12 ⁴Fred Hutchinson Cancer Research Center, Human Biology Division, Seattle, USA.

13

14 **Corresponding author:** Prof. Jochen H. M. Prehn, Department of Physiology and Medical Physics,
15 Royal College of Surgeons in Ireland, 123 St. Stephen's Green, Dublin 2, Ireland. Tel.: +353-1-402-
16 2255; Fax: +353-1-402-2447; E-mail: prehn@rcsi.ie

17

18 **Running Title:** Transcriptomic-dependent *Fn/Fusobacteriales* impact.

19 **Key words:** colorectal cancer, *Fusobacterium nucleatum*, *Fusobacteriales*, microbiome, molecular
20 subtypes and signatures, CMS, CRIS, mesenchymal biology, immune involvement, multi-omics
21 integration, prognostic biomarker.

Word counts: 247 words for the abstract and 3630 words for the main manuscript.

23 **Abstract (247 words)**

24 **Objective.** Transcriptomic-based subtyping, Consensus Molecular Subtyping (CMS) and CRC
25 Intrinsic Subtyping (CRIS), identify a patient subpopulation with mesenchymal traits (CMS4/CRIS-B)
26 and poorer outcome. Here, we investigated the relationship between prevalence of *Fusobacterium*
27 *nucleatum* (*Fn*) and *Fusobacteriales*, CMS/CRIS subtyping, cell type composition, immune infiltrates
28 and host contexture to refine patients stratification and identify druggable context-specific
29 vulnerabilities.

30 **Design.** We coupled cell culture experiments with characterization of *Fn/Fusobacteriales* prevalence
31 and host biology/microenviroment in tumours from 2 independent CRC patient cohorts (Taxonomy:
32 n=140; TCGA-COAD-READ: n=605).

33 **Results.** *In vitro*, *Fn* infection induced inflammation via NF κ B/TNF α in HCT116 and HT29 cancer cell
34 lines. In patients, high *Fn/Fusobacteriales* were found in CMS1, MSI tumours, with infiltration of
35 macrophages M1, reduced macrophages M2, and high IL6/IL8/IL1 β signaling. Analysis of the
36 Taxonomy cohort suggested that *Fn* was prognostic for CMS4/CRIS-B patients, despite having lower
37 *Fn* load than CMS1 patients. In the TCGA-COAD-READ cohort, we likewise identified a differential
38 association between *Fusobacteriales* relative abundance and outcome when stratifying patients in
39 mesenchymal (either CMS4 and/or CRIS-B) vs. non-mesenchymal (neither CMS4 nor CRIS-B).
40 Patients with mesenchymal tumours and high *Fusobacteriales* had approximately 2-fold higher risk of
41 worse outcome. These associations were null in non-mesenchymal patients. Modelling the 3-way
42 association between *Fusobacteriales* prevalence, molecular subtyping, and host contexture with logistic
43 models with an interaction term disentangled the pathogen/host-signaling relationship and identified
44 aberrations (including EMT/WNT/NOTCH) as candidate targets.

45 **Conclusion.** This study identifies CMS4/CRIS-B patients with high *Fn/Fusobacteriales* prevalence as
46 a high-risk subpopulation that may benefit from therapeutics targeting mesenchymal biology.

47 **Significance of this study**

48 **What is already known on this subject?**

49 • *Fusobacterium nucleatum* (*Fn*), a commensal Gram-negative anaerobe from the *Fusobacteriales*
50 order, is an onco-bacterium in CRC as a causal relationship between *Fn* prevalence and CRC
51 pathogenesis, progression and treatment response has been reported *in vivo*.
52 • Broad spectrum antibiotics has proven moderately successful in reducing tumour growth in
53 preclinical models. However, the use of antibiotics to treat bacterium-positive cases in the clinic is
54 not a viable option as it may further alter the already dysbiotic gut microbiome of CRC patients and
55 may also have limited efficacy against *Fn* which penetrates and embeds deeply within the tumour.
56 • The highly heterogenous CRC patient population can be classified into distinct molecular subtypes
57 (CMS and CRIS) based on gene expression profiles mirroring the underlying transcriptional
58 programs. Patients classified as CMS4 and CRIS-B exhibit a mesenchymal phenotype and have
59 poorer outcome.

60

61 **What are the new findings?**

62 • *Fn/Fusobacteriales* prevalence is associated with immune involvement (decrease in macrophages
63 M1 and increase in macrophages M2) and activation of specific signalling programs (inflammation,
64 DNA damage, WNT, metastasis, proliferation, cell cycle) in the host tumours.
65 • The prevalence of bacteria from the *Fusobacteriales* order, largely driven by *Fn* species, play an
66 active or opportunistic role depending on the underlying host tumour biology and
67 microenvironment.
68 • *Fn* and other species of the *Fusobacteriales* order are enriched in CMS1 (immuno, microsatellite
69 unstable) patients compared to CMS2-4 cases.
70 • *Fn/Fusobacteriales* prevalence is associated with worse clinical outcome in patients with
71 mesenchymal-rich CMS4/CRIS-B tumours, but not in patients with other molecular subtypes.

72

73

74 **How might it impact on clinical practice in the foreseeable future?**

75 • *Fn/Fusobacteriales* screening and transcriptomic-based molecular subtyping should be considered to
76 identify patients with mesenchymal-rich tumours and high bacterium prevalence and to inform
77 disease management.

78 • *Fn/Fusobacteriales* prevalence may need to be addressed exclusively in patients with mesenchymal-
79 rich high-stromal infiltrating tumours rather than a blanket-approach to treat all pathogen-positive
80 patients.

81 • Clinical management of the disease for this subpopulation of high-risk patients with unfavourable
82 clinical outcome could be attained by administering compounds currently in clinical trials that target
83 aberrations in the host signaling pathways (NOTCH, WNT, EMT) and tumour microenviroment
84 (inflammasome, activated T cells, complement system, and macrophage chemotactism and
85 activation).

86 **Introduction (395 words)**

87 Colorectal cancer (CRC) has one of the highest morbidities and mortality rates among solid cancers
88 and its incidence is steadily on the rise accounting for circa 10% of newly diagnosed cancer cases
89 worldwide [1]. CRC patients with similar macroscopic clinico-pathological characteristics exhibit a
90 high degree of heterogeneity at the molecular level, which translates into heterogeneous and often sub-
91 optimal response to treatment. Thus, research has focussed on molecular subtyping strategies based on
92 single or multi-omics data from the host to categorise patients into subgroups to aid in risk stratification
93 and disease management. Subtyping strategies such as the Consensus Molecular Subtyping (CMS, [2])
94 and the Colorectal Cancer Intrinsic Subtyping (CRIS, [3]) classify patients into subgroups with more
95 homogeneous signaling features based on key transcriptomic programs. Among the four subtypes
96 identified by the CMS classifier, CMS4 patients have high stroma infiltration along with up-regulated
97 angiogenesis and Transforming Growth Factor- β (TGF β) signaling and show poorer recurrence-free
98 and overall survival [2]. Similarly, CRIS-B patients feature mesenchymal traits and also exhibit poorer
99 outcome compared to patients classified as CRIS-A, CRIS-C-E [3].

100 Recent research has identified the microbiome as a key player in health and disease, including cancer
101 [4]. Several research groups, including ours, have shown that *Fusobacteriales*, largely from
102 *Fusobacterium nucleatum* (*Fn*), are more abundant in tumour tissue compared to matched adjacent
103 mucosa [5] suggesting a causative role in CRC progression [12]. More advanced, right-sided, MSI
104 tumours are typically enriched with *Fn* [9]. Remarkably, anti-microbial treatment has been shown to
105 reduce tumour burden in mouse xenograft models [10], corroborating the association between *Fn*-
106 positive patients and poorer outcome observed in some studies [5]. However, the prognostic value of
107 *Fn* prevalence was not observed in other cohort studies (reviewed in [16]). Thus, we hypothesized that
108 the impact of *Fn/Fusobacteriales* may differ according to the underlying tumour biology.

109 In this study, we combined mechanistic *in vitro* experiments in colon cancer cells with an in-depth
110 analysis in 2 independent CRC patient cohorts and a systematic multi-*omic* characterization of cell
111 signalling and tumour microenvironment in n=745 patients to investigate the interaction between the

112 dysregulation induced by *Fusobacteriales*, including *Fn*, prevalence on the human host and conversely,
113 the characteristics of the host microenvironment that allow pathogens to thrive. Here, we provide
114 evidence that the prognostic value of *Fn/Fusobacteriales* strongly relates to the molecular subtype of
115 the host tumour and is confined to subtypes showing mesenchymal involvement.

116 **Results (2253 words)**

117 ***Fusobacterium nucleatum* infection induces inflammation mediated by TNF α and NF κ B in CRC
118 cellular cultures**

119 Due to the presence of *Fusobacterium nucleatum* (*Fn*) in CRC tumour tissue [5], a causative role for
120 this bacterium to exacerbate tumourigenesis has been put forward. Infection of colon cells with *Fn* has
121 previously been shown to induce inflammation, activate NF κ B signaling and increase expression of the
122 pro-inflammatory cytokine tumour necrosis factor alpha (TNF α) [18], (Fig. 1A). Hence, we infected
123 HCT116 and HT29 colon cancer cell lines cultures for 6 hours to assess epithelial cell response to
124 increasing amounts of *Fn* (multiplicity of infection, MOI, bacteria-to-cancer-cells 10, 100 and 1000).
125 We found that NF κ B signaling was indeed activated upon infection with *Fn* in CRC cell lines, as
126 evidenced through the degradation of I κ B α (alpha nuclear factor of kappa light polypeptide gene
127 enhancer in B cells inhibitor) (Fig. 1B), an increase in NF κ B transcriptional activity (Fig. 1C) and, a
128 marked increase in mRNA expression of the NF κ B target gene, TNF α (Fig. 1D). Taken together, these
129 results confirm that *Fn* co-culture with human colon cancer epithelial cells promotes a pro-
130 inflammatory response.

131

132 **Prevalence of *Fn* and *Fusobacteriales* in tumour resections**

133 Next, we sought to investigate the relationship between inflammation in the human host and prevalence
134 of *Fn* and *Fusobacteriales* in tumour resections of CRC patients. We selected an in-house multi-center
135 stage II-III cohort (Taxonomy, n=140, [19], [20]) and the colon (COAD) and rectal (READ) cases of
136 The Cancer Genome Atlas cohort (TCGA-COAD-READ, n=605 patients, Fig. 2A) to encompass the
137 heterogeneity of the CRC clinico-pathological characteristics observed in the clinic. Demographic,
138 clinico-pathological characteristics for the Taxonomy and TCGA-COAD-READ cohorts are
139 summarised in Suppl. Table 1. We determined *Fn* abundance by a targeted quantitative real-time
140 polymerase chain reaction (qPCR) in tumour resections of the Taxonomy cohort where we detected *Fn*

141 in n=101 of 140 (72%) patients (**Fig. 2B**). The distribution of *Fn* positivity levels (relative to the human
142 PGT gene) was heterogeneous and we categorized patients as *Fn*-high or *Fn*-low using the 75th
143 percentile as cut-off (**Fig. 2B**). We estimated *Fusobacteriales* relative abundance (RA) in the TCGA-
144 COAD-READ cohort from RNA sequencing data by mapping non-human reads to microbial reference
145 databases and retaining only high-quality matches (see **Methods**) with a PathSeq analysis [21], (**Fig.**
146 **2A**). For downstream analyses, we reported the relative abundance (RA) at the order, family, genus and
147 species taxonomic rank and expressed it as percentage of the total bacterial abundance. We detected
148 *Fusobacteriales* (defined as RA over zero, at the order level) in n=558 of 605 (92%) of the TCGA-
149 COAD-READ patients, (**Fig. 2D**). *Fn* was the most abundant species and was detected in 82% of the
150 TCGA-COAD-READ patients (compared to 72% in the Taxonomy cohort), accounting on average for
151 approximately 45% of total *Fusobacteriales* RA and accounting for over 75% of total *Fusobacteriales*
152 RA in 16% of cases (**Fig. 2C**). Analogously to the Taxonomy cohort, we categorized patients as
153 *Fusobacteriales*-high or *Fusobacteriales*-low using the 75th percentile as cut-off.

154
155 **Higher *Fn* and *Fusobacteriales* prevalence correlates with inflammation and immune
156 involvement**

157 We examined the association between host gene expression profiles of key markers shown to
158 orchestrate inflammation and either *Fn* load or *Fusobacteriales* RA in the Taxonomy and TCGA-
159 COAD-READ cohorts, respectively. In line with the *in vitro* experiments (**Fig. 1**), we detected an
160 increase in NFKB1 and a trend in TNF α gene expression, recapitulated by transcriptomic-based
161 signatures for an overall inflammation status (TIS) mediated by the cytolytic and interferon (IFN γ)
162 pathways in the Taxonomy cohort (**Fig 2E**). When investigating further key inflammation players, we
163 observed a marked increase in pro-inflammatory interleukins (IL6, IL8, IL10, IL1 β , IL13),
164 cytokines/chemokines (CCL8, CSF1, ICAM1), metallo-proteins (MMP1, MMP3, MMP9), NOS2, the

165 inflammasome complex (NLRP3) and COX2 in *Fn*-high vs. -low Taxonomy patients (**Fig. 2E** and
166 **Suppl. Fig. 1**).

167 Next, we sought to validate and build upon our findings from the in-house Taxonomy cohort by
168 analyzing the TCGA-COAD-READ cohort (**Fig. 2F**). At the transcription level, we confirmed an
169 exacerbated inflammatory state when comparing *Fusobacteriales*-high and -low patients mediated by
170 the NF κ B-TNF α axis, IFN γ with cytolytic involvement. *Fusobacteriales*-high patients overexpressed
171 pro-inflammatory interleukins (IL6, IL8, IL10, IL1 β), cytokines/chemokines (CCL8, ICAM1), metallo-
172 proteinases (MMP1, MMP3), NOS2 and inflammasome markers (NLRP3), (**Fig. 2F**).

173 As inflammation is strongly tied to immune cell migration and activity, we next investigated whether
174 there was a link between immune cell composition and either *Fn* load (Taxonomy) or *Fusobacteriales*
175 RA (TCGA-COAD-READ). Cell composition was computationally deconvoluted from gene
176 expression profiles with quanTiseq [23] and MCP-Counter [24], (**Fig. 2G-H**). Despite observing high
177 inter-patient heterogeneity in cell composition within the Taxonomy and TCGA-COAD-READ
178 cohorts, we robustly detected higher immune cell activation and polarization when comparing patients
179 with high vs. low *Fn* load (Taxonomy) or *Fusobacteriales* RA (TCGA-COAD-READ). Patients with
180 high *Fn* load (Taxonomy) or *Fusobacteriales* (TCGA-COAD-READ) showed higher predicted
181 abundance of regulatory T cells (T regs) coupled with an increase in M1 macrophages and decrease in
182 M2 macrophages (**Fig. 2I**). MCP-counter identified a strong positive association between neutrophil
183 infiltration and either *Fn* load (Taxonomy) or *Fusobacteriales* RA (TCGA-COAD-READ), (**Fig. 2I**).
184 However, no difference in predicted neutrophils abundance was detected by quanTiseq. Importantly,
185 no difference in fibroblasts and endothelial cells was observed by *Fn/Fusobacteriales* in either cohort
186 by either method (**Fig. 2I**).

187

188 **Multi-omic characterization of the association between *Fusobacteriales* relative abundance and**
189 **human host tumour microenvironment in the TCGA-COAD-READ cohort**

190 We next leverage the rich molecular characterization of the TCGA-COAD-READ cohort to perform a
191 systematic and unbiased characterization of the association between *Fusobacteriales* RA and patient
192 clinical and molecular features to identify human host vulnerabilities that may be conducive for tumour
193 development (**Fig. 3**).

194 We observed higher *Fusobacteriales* in patients of older age, diagnosed with more advanced disease
195 stage and tumours located in the colon, particularly in proximal sites, (**Fig 3A**), corroborating studies
196 assessing *Fn* [13]. In contrast, we found no statistically significant differences in *Fusobacteriales* RA
197 by sex, body mass index and neither lymphovascular nor perineural invasion (**Sup. Fig. 2**).

198 Patients harbouring higher *Fusobacteriales* showed lower genomic intra-tumour heterogeneity, had
199 higher silent and non-silent mutational burden and were enriched in microsatellite unstable cases, (**Fig**
200 **3B**). *Fusobacteriales*-high patients showed an increase in transitions, defined as the exchange of two-
201 ring purines (A↔G) or of a one-ring pyrimidines (C↔T), coupled with a decrease in transversions, a
202 substitution of purine for pyrimidine bases (**Suppl. Fig. 3A**) as evidenced by a decrease in conversion
203 changes of C>G and T>A, (**Suppl. Fig. 3B**). We found no difference in prevalence of common
204 mutations in CRC by *Fusobacteriales* (high vs. low) except for BRAF (**Fig. 3C**). BRAF mutations
205 tended to be more common among *Fusobacteriales*-high patients, as observed when assessing *Fn* [13].
206 A comprehensive screen revealed that mutations in cell cycle (ATM), Hedgehog signaling (MEGF8),
207 DNA damage/repair (TRIP12, PRKDC), mitotic spindle (ASPM), migration/adhesion (TRIO, GPR98)
208 were more prevalent in *Fusobacteriales*-high patients, (**Fig. 3D, Suppl. Table 2**).

209 Next, we set out to investigate the relationship between copy number alterations (CNAs) and
210 *Fusobacteriales* presence in the TCGA-COAD-READ cohort (**Fig. 3E-G**). We determined recurrent
211 CNAs amplifications and deletions across the whole cohort by applying the GISTIC algorithm [26]
212 (**Sup. Figs. 4-5** and **Suppl. Table 3**). *Fusobacteriales*-high cases showed lower chromosomal
213 instability with a lower fraction of the genome affected by recurrent CNAs, in line with their MSI

214 unstable status. Next, we identified CNA amplifications (in red) or deletions (in blue) whose frequency
215 of occurrence differed when comparing *Fusobacteriales*-high vs. -low patients and thus may be
216 specifically associated with the bacterium presence (**Fig. 3F**). CNAs more frequently (>15%) observed
217 in *Fusobacteriales*-high vs. low cases included deletions in 8p23.2 (tumour suppressor CSMD1 and
218 LOC100287015); 18q21.1 (MIR4743 and RNA binding by CTIF) and 18q23 which impacts the
219 regulation of interleukin-6 and chemokine secretion, cell-cell adhesion and host of viral transcription,
220 as determined by enrichment analyses carried out with EnrichR, (**Fig. 3G**).
221 We then focused on the transcriptional level and we combined enrichment analyses with pathway-
222 activity signatures to compare cellular processes by *Fusobacteriales* RA (**Fig. 3H-L**). Transcriptional
223 profiles differed by mTORC1 and Myc signalling, cell cycle (G2-M checkpoint), mitotic spindle,
224 epithelial-to-mesenchymal transition, TGF β and interleukin-1 regulation of extracellular matrix, matrix
225 remodelling including focal adhesion, cytoskeleton and contractile actin filament bundle, mitochondrial
226 translational elongation/termination and protein complex assembly and stromal estimates (**Fig. 3H-I**,
227 **Sup. Fig. 6** and **Sup. Table 4**). We corroborated these findings by comparing the activation of
228 signalling pathways estimated by gene set signatures identified in the literature (see **Methods**) in
229 *Fusobacteriales*-high vs. low patients. Indeed, *Fusobacteriales* presence was positively associated with
230 proliferation, WNT, metastasis (**Fig. 3L**) and DNA damage.
231 Next, we sought to investigate whether the findings at the genomic and transcriptional level were also
232 observed in protein profiles determined by Reverse Phase Protein Array (RPPA). We found a
233 differential expression by *Fusobacteriales* RA for proteins involved in microenvironment composition
234 (Claudin7), cell cycle (Cycline1), apoptosis (cleaved Caspase7), proliferation (DLV3), Hippo pathway
235 (Yap), DNA damage (Chk1, ATM), receptor and MAP kinases and PI3K signalling, (**Fig. 3M-O**, **Sup.**
236 **Fig. 7** and **Sup. Table 5**).
237

238 ***Fn* and *Fusobacteriales* prevalence differs by transcriptomic-based molecular subtype**

239 The systematic screen above pinpointed host aberrations by *Fusobacteriales* prevalence that are
240 hallmark by transcriptomic-based molecular subtypes. Hence, we classified patients in the study by
241 CMS [2] and CRIS [3] subtyping. We observed higher *Fn* load (Taxonomy, **Fig. 4A**) and
242 *Fusobacteriales* RA (TCGA-COAD-READ, **Fig. 4C**) in CMS1 tumours, corroborating the interplay
243 between pathogen prevalence and host immunity. Moreover, we observed higher *Fn* load in CRIS-B
244 tumours (**Fig. 4B**) and *Fusobacteriales* RA in CRIS-A cases (**Fig. 4D**) of the Taxonomy and TCGA-
245 COAD-READ cohorts, respectively. At the family rank, *Fusobacteriaceae* were more abundant than
246 *Leptotrichiaceae* accounting for 77% and 23% of total *Fusobacteriales* RA and ~2% and ~<1% of the
247 total bacteria RA, respectively. In line with the findings at the order level, we observed an increase in
248 *Fn*, the most abundant *Fusobacterium* species, in CMS1 and CRIS-A cases (**Fig. 4E-F**). In line with
249 the findings at the order level, we observed an approximately 3-fold increase when comparing patients
250 classified as CMS1 vs. the rest (**Fig 4E**). *Fn*, the most abundant *Fusobacterium* species, was enriched
251 in CMS1 and CRIS-A cases (**Fig. 4E-F**). Next, we examined whether the positive association between
252 inflammation and immune involvement by *Fn/Fusobacteriales* presence could be ascribed to the host
253 CMS1 milieu or whether there was an additional pathogen-induced component. When restricting the
254 analysis to CMS1 cases, we observed higher expression of pro-inflammatory markers in
255 *Fusobacteriales*-high patients of the TCGA-COAD-READ cohort. We detected no association between
256 pathogen prevalence and expression of anti-inflammatory markers or inflammation signatures in
257 neither CRC cohorts (**Fig. 4G-H**). Taken together these results suggest that *Fn/Fusobacteriales* may
258 play an active role in mediating inflammation in the host.

259

260 **Patients with high *Fn/Fusobacteriales* have worse outcome in CMS4/CRIS-B**

261 Next, we sought to investigate whether bacterium presence correlated with patient clinical outcome
262 assessed by overall- (OS), disease-specific- (DSS) and disease-free- (DFS) survival endpoints (**Fig. 5**
263 and **Suppl. Figs. 8-10**).

264 We found no statistically significant differences in neither cohort when comparing survival curves from
265 patients grouped by either *Fn* load or *Fusobacteriales* RA (**Fig. 5A, E, I** and **Suppl. Figs. 8-10**). We
266 hypothesized that *Fn/Fusobacteriales* may result in poorer outcome in a subtype-dependent context.
267 Indeed, we identified a differential association between *Fusobacteriales* RA and clinical outcome of
268 the TCGA-COAD-READ cohort in mesenchymal (either CMS4 and/or CRIS-B) vs. non-mesenchymal
269 (neither CMS4 nor CRIS-B) tumours, (**Fig. 5G, H, K, L** and **Sup. Figs. 8-10**). *Fusobacteriales*-high
270 mesenchymal patients had approximately 2-fold higher risk of worse outcome while these associations
271 were null in non-mesenchymal patients (**Fig. 5G, H, K, L** and **Sup. Figs. 8-10**).

272 Although numbers in the Taxonomy cohort are limited, when restricting the analysis to CMS4 and/or
273 CRIS-B cases, we observed a trend whereby *Fn*-high patients had shorter OS than those with low *Fn*
274 load. Again, no difference in survival curves by *Fn* load was observed in non-mesenchymal Taxonomy
275 patients (**Fig. 5C-D**).

276 Exploratory analyses examining the association between clinical outcome and pathogen prevalence at
277 taxonomic ranks of increasing resolution (order, family, genus and species) in the TCGA-COAD-
278 READ cohort by fitting Cox regression models on the whole unselected population and in
279 mesenchymal vs. non-mesenchymal settings revealed that the prognostic impact stems primarily from,
280 but is not limited to, species, including *Fn*, from the *Fusobacterium* genus from the *Fusobacteriaceae*
281 family (**Fig. 5M** and **Sup. Fig. 10**).

282

283 **Putative mechanisms underlying selective *Fusobacteriales* virulence in mesenchymal tumours**

284 We examined the host signaling pathways and microenvironment to identify alterations that may be
285 mediated by and/or exacerbated by *Fusobacteriales* (i.e. interact) and, thus, may promote virulence
286 and, ultimately, result in an unfavorable clinical outcome. To disentangle the 3-way association
287 between *Fusobacteriales* RA, gene/signature, and molecular subtyping, we fitted 2 distinct logistic
288 regression models for each feature of interest in the TCGA-COAD-READ cohort. The selection of

289 features was hypothesis-driven and included key host signaling pathways and immuno-modulators
290 (**Fig. 6A**).

291 **Fig. 6A** reports adjusted P-values from the 2 models capturing the association between *Fusobacteriales*
292 RA (high vs. low) and either each gene/signature (**model 1**: *Fusobacteriales* ~ *gene/signature*, x-axis)
293 or the interaction between each gene/signature with the molecular subtype (**model 2**: *Fusobacteriales* ~
294 *gene/signature:molecular subtype*, y-axis). The top right half quadrant (darker gray shaded area)
295 identifies a set of genes/signatures whose expression patterns differ by molecular subtype (statistically
296 significant interaction p-value in model 2) and thus may be mediating the pathogenic impact of
297 *Fusobacteriales* and were prioritized for downstream analyses (**Fig. 6B**).

298 NOTCH, EMT, TIS score, IL6, CSF1 are among the genes/signatures identified by model 2 in **Fig. 6A**
299 whose expression profiles track with molecular subtyping and may represent druggable vulnerabilities
300 in patients with mesenchymal tumours and high *Fn/Fusobacteriales* prevalence and ameliorate clinical
301 outcome (**Fig. 6B**).

302 **Discussion (952 words)**

303 *Fusobacteriales*, predominantly *Fn*, have been associated [5] with pathogenesis, progression and
304 treatment response in CRC. We coupled mechanistic studies in cell cultures with hypothesis-driven and
305 unbiased screening in clinically-relevant and 'omics-rich CRC cohorts to examine the cross-talk
306 between pathogen-host and pathogen-tumour microenvironment. We demonstrated relationships
307 between *Fn/Fusobacteriales* prevalence with host immune, signaling activation and transcriptomic-
308 based molecular subtypes. Our findings suggest that host-pathogen interactions can define patient sub-
309 populations where *Fn/Fusobacteriales* play an active or opportunistic role depending on the underlying
310 host tumour biology and microenvironment and identify putative druggable and clinically-actionable
311 vulnerabilities.

312 We observed higher *Fn/Fusobacteriales* prevalence in CMS1 patients, corroborating findings by
313 Purcell [28]. Interestingly, we found that higher pathogen prevalence did not correlate with poorer
314 disease outcome. In contrast, *Fn/Fusobacteriales* virulence was exacerbated in CMS4/CRIS-B patients,
315 suggesting that pathogen persistence may need addressing exclusively in mesenchymal-rich high-
316 stromal infiltrating tumours and arguing against a blanket-approach to treat all pathogen positive
317 patients. Treatment with wide spectrum antibiotics reduces the growth of *Fn*-positive tumours *in vivo*
318 [10]. However, the use of antibiotics to treat *Fn*-positive CRC tumours may be limited as *Fn* penetrate
319 deeply within tumour, immune and endothelial cells where they internalize with endosomes and
320 lysosomes [29], adapt [30] and persist [10]. In addition, long-term use of antibiotics can cause
321 dysbiosis.

322 Given that “it takes two to tango”, namely a high pathogen prevalence and a conducive host milieu, we
323 further examined this interdependence to identify druggable aberrations in the host signaling pathways
324 and microenvironment. We identified putative targets related to (pro-)inflammation, inflammasome,
325 activated T cells, complement system, metallo-proteins and macrophage chemotaxis and activation.
326 *Fusobacteriales* induce a constitutively activated NF- κ B-TNF α -IL6 state which results in activation of
327 metallo proteins and inflammatory cytokines (CSF1-3) which mediate macrophage differentiation,

328 inhibit cytotoxic immune cells and promote proliferation of myeloid-derived-suppressor (MDSC) cells.
329 Indeed, we observed an increase in inflammation and macrophages M1 and decrease in macrophages
330 M2 in patients with higher *Fn/Fusobacteriales* prevalence. We envisage that therapeutic options, such
331 as NLRP3/AIM2 inflammasome suppression [31], IL1 β blockade [32], TNF α [33] or IL6 inhibition
332 [34], that have been approved for treatment of chronic inflammation and cytokines storm syndrome in
333 multiple cancers, rheumatoid arthritis and COVID-19 may ameliorate the immunosuppressive
334 microenvironment induced by *Fn/Fusobacteriales*.
335 Importantly, these targets are involved in not only promoting an immunosuppressive microenvironment
336 by recruiting tissue-associated macrophages (TAMs) and MDSCs, but also in orchestrating invasion,
337 angiogenesis, epithelial-to-mesenchymal transition and, ultimately, metastasis. The pro-metastatic role
338 of *Fn/Fusobacteriales* is further corroborated by findings in the literature linking higher pathogen
339 prevalence in more-advanced disease stage and metastasis in clinical specimens [5] and higher
340 metastatic burden in mice inoculated with *Fn* [35].
341 Cancer cells with an EMT phenotype secrete cytokines such as IL10 and TGF β that can further
342 promote an immunosuppressive microenvironment. Additionally, secretion of IL6 and IL8 from stroma
343 cells can further foster an EMT phenotype, activate primary fibroblasts (carcinoma-associated
344 fibroblast, CAFs) which, in turn, may promote angiogenesis and invasion [36]. Taken together, these
345 aberrations may result in a self-reinforcing mechanism that confers on cancer cells the ability to
346 migrate, invade the extracellular matrix, extravasate and seed metastasis. Indeed, when comparing the
347 transcriptomic profiles by *Fusobacteriales* RA in the TCGA-COAD-READ cohort, we identified
348 dysregulation affecting cell architecture involving apical surface dynamics and Aurora A kinase
349 signaling, which regulate cMyc, DNA repair, cell motility/migration and induce EMT transition via β -
350 catenin and TGF β leading to metastasis and resistance to treatment in multiple cancer types [37]. Small
351 molecule inhibitors against aurora A have shown encouraging results in preclinical studies and clinical
352 trials in CRC [38] and other cancers [39]. Cytoskeleton shape, filopodium protrusions and alterations in
353 cell adhesion and structure are hallmark of extracellular matrix invasion. EMT key effectors, SNAIL

354 and ZEB1, alter apical surface dynamics by inhibiting scaffolding proteins and by inducing expression
355 of matrix metalloproteins (MMP3, MMP9), resulting in loosened tight-junctions, altered cell polarity
356 and increased plasticity which, in turn, enable cell invasion [40]. Dysregulations in MMPs expression
357 may aid cancer cells that have reached the bloodstream to extravasate to distant tissues [41] by priming
358 the vascular endothelium via upregulation of VEGF-A [42] and by increasing permeability via COX2
359 upregulation [43]. Our analyses in the TCGA-COAD-READ cohort identified higher expression of
360 VEGF as well as an angiogenesis signature and COX2 in patients with higher *Fusobacteriales* RA.
361 MMPs treatment with a new generation of selective and highly penetrative inhibitors [44] is being
362 trialed in gastrointestinal cancers [45] and Mehta reported lower *Fusobacteriales* RA in subjects treated
363 with Aspirin, a COX2 inhibitor [46].

364 Green [47] demonstrated that MAPK7 is a master regulator of MMP9 and promotes the formation of
365 metastasis. Indeed, we observed a dysregulation in MAPK signaling at the protein level when
366 comparing *Fusobacteriales*-high vs. -low patients of the TCGA-COAD-READ cohort. MAPK7
367 induces EMT transition, cell migration and regulates TAMs polarization in a metallo proteins-
368 dependent manner [47], rendering it an appealing upstream therapeutic target. IL6 orchestrates MAPK-
369 STAT3 signaling which in turn regulates the dynamic transition between 2 CAFs sub-populations,
370 EMT-CAFs and proliferation-CAFs [48], rendering the IL6-TGF β -EMT-CAFs cross-talk a valid
371 therapeutic target. While targeting directly EMT via NOTCH or WNT has shown limited success in the
372 clinic [49], microenvironment remodeling to reverse immunosuppression by inhibiting CXCL12 [50]
373 or promoting T-cell infiltration [51] or function via engineered oncolytic adenovirus [52], has shown
374 has shown promising results in reducing metastasis formation [53]. Additionally, we observed a
375 positive correlation between gene expression of IL8, CXCL8, CXCR1 and CXCL10 and
376 *Fn/Fusobacteriales* prevalence, corroborating findings from Casasanta assessing *Fn* in HCT116 CRC
377 cells [54].

378 In conclusion, our analyses have identified a patient sub-population that has an unfavorable clinical
379 outcome when their tumours exhibit mesenchymal traits and are highly positive with

380 *Fn/Fusobacteriales* and pinpointed clinically-actionable host-specific vulnerabilities that suggest new
381 treatments for these patients that extend beyond broad spectrum antibiotics.

382 **Materials and Methods (30 words)**

383 Detailed methods for the *in vitro* cell culture experiments and the study design, cohorts description and
384 analysis steps are provided in the online supplementary materials and methods.

385

386 **Patient and public involvement statement**

387 Patients or the public were not involved in the design, recruitment, conduct, reporting and
388 dissemination of this research.

389

390 **Data availability**

391 Processing and analysis code along with pathogen prevalence with corresponding clinical and
392 molecular datasets for the Taxonomy and TCGA-COAD-READ cohorts included in this study will be
393 made publicly available and archived upon publication at Zenodo (<https://10.5281/zenodo.4019142>).

394 Pathogen prevalence will include *Fusobacterium nucleatum* load and *Fusobacteriales* relative
395 abundance (along with higher resolution estimates at genus, family and species taxonomic rank) for the
396 Taxonomy and TCGA-COAD-READ cohorts, respectively.

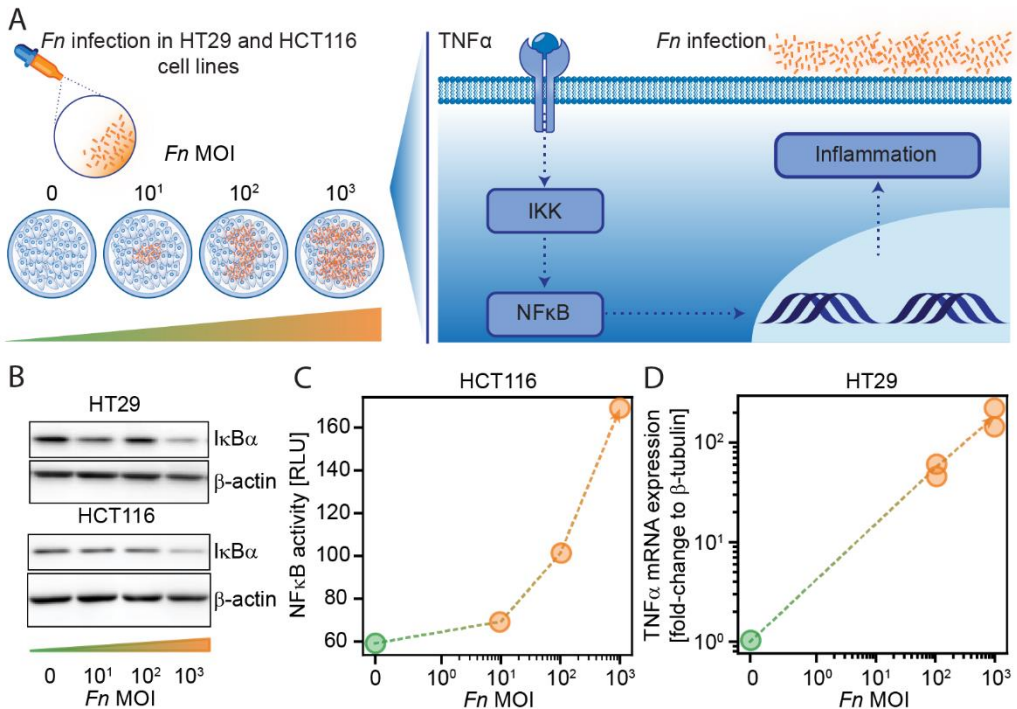
397

398 **Acknowledgments**

399 We wish to thank the patients who kindly donated their samples and made this study possible. This
400 study was supported by a grant from the Health Research Board and Science Foundation Ireland to
401 JHMP (16/US/3301), a studentship to KS sponsored by The Northern Ireland Department for the
402 Economy (NI DfE), and by funding from NI DfE (SFI-DEL 14/1A/2582; STL/5715/15). The results
403 included here are in part based upon data generated by the TCGA Research Network:
404 <https://www.cancer.gov/tcga>. We wish to acknowledge the Information Technology department at the
405 Royal College of Surgeons in Ireland and the DJEI/DES/SFI/HEA Irish Centre for High-End
406 Computing (ICHEC) for the provision of computational facilities and support.

407 **Figures**

408 **Figure 1.**



409

410 **Fn infection induces inflammation mediated by TNF α and NF κ B in HCT116 and HT29 CRC cell**
411 **lines.**

412 **A.** Schematic representation of the experimental setup to investigate how *Fn* may trigger inflammation
413 via TNF α and NF κ B signalling pathways.

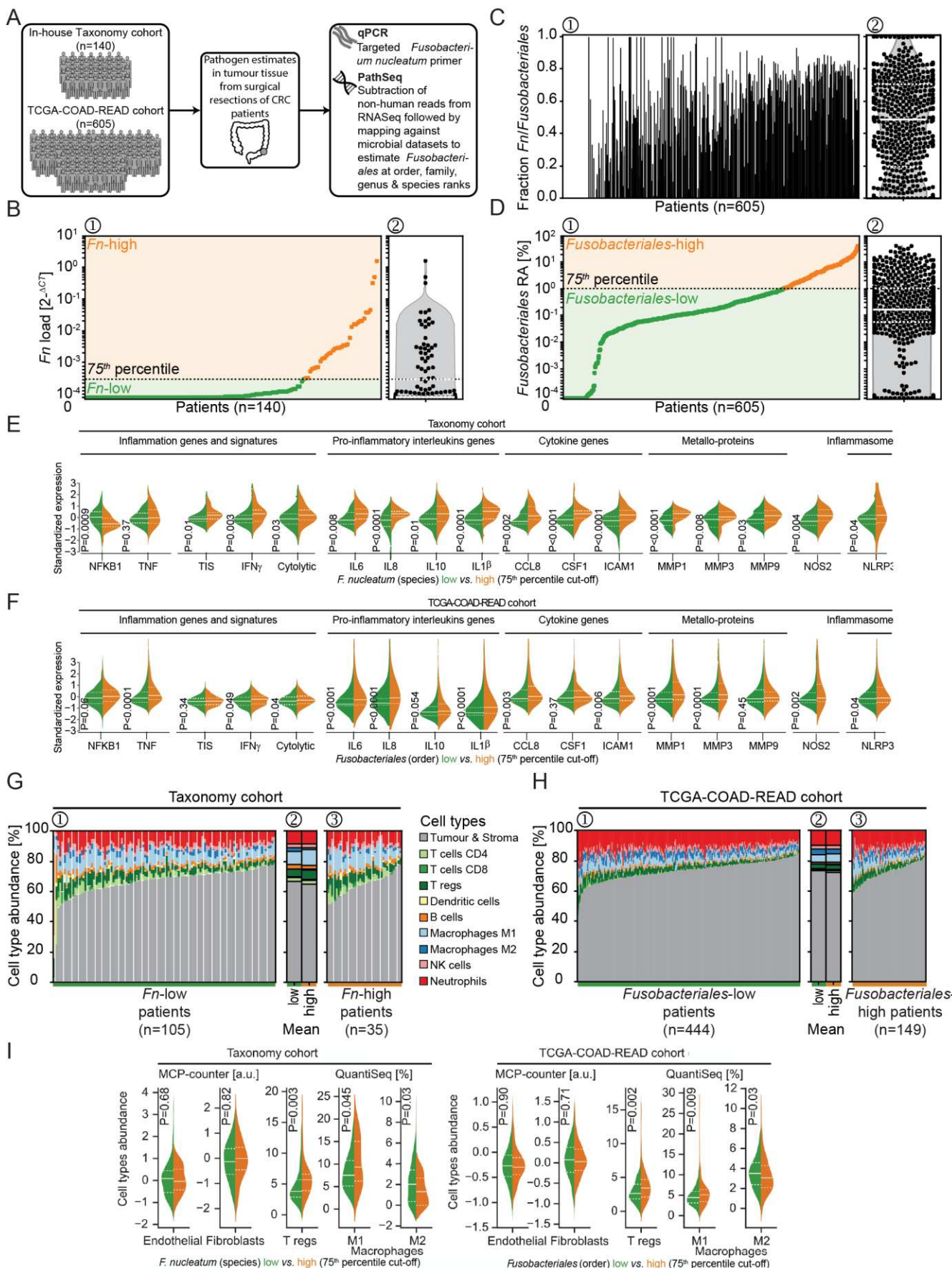
414 **B.** Western blot analysis of I κ B α and β -actin in HT29 and HCT116 cell cultures following infection
415 with *Fn* (MOI bacteria-to-cancer-cells 10, 100 and 1000).

416 **C.** NF κ B transcriptional activity assay in HCT116 cells 6h following infection with *Fn* (MOI bacteria-
417 to-cancer-cells 100 and 1000).

418 **D.** TNF α mRNA expression relative to β -tubulin in HT29 cells 6h following infection with *Fn* (MOI
419 bacteria-to-cancer-cells 100 and 1000).

420 Panels **B-D** show representative results from duplicate experiments.

Figure 2.



423 ***Fn/Fusobacteriales prevalence is associated with inflammation and immunosuppression in CRC***
424 ***patients of the Taxonomy and TCGA-COAD-READ CRC cohorts.***

425 **A.** Schematic representation of the cohorts included in the study and methods to estimate *Fn* load and
426 *Fusobacteriales* (order) relative abundance in the Taxonomy and TCGA-COAD-READ cohorts,
427 respectively.

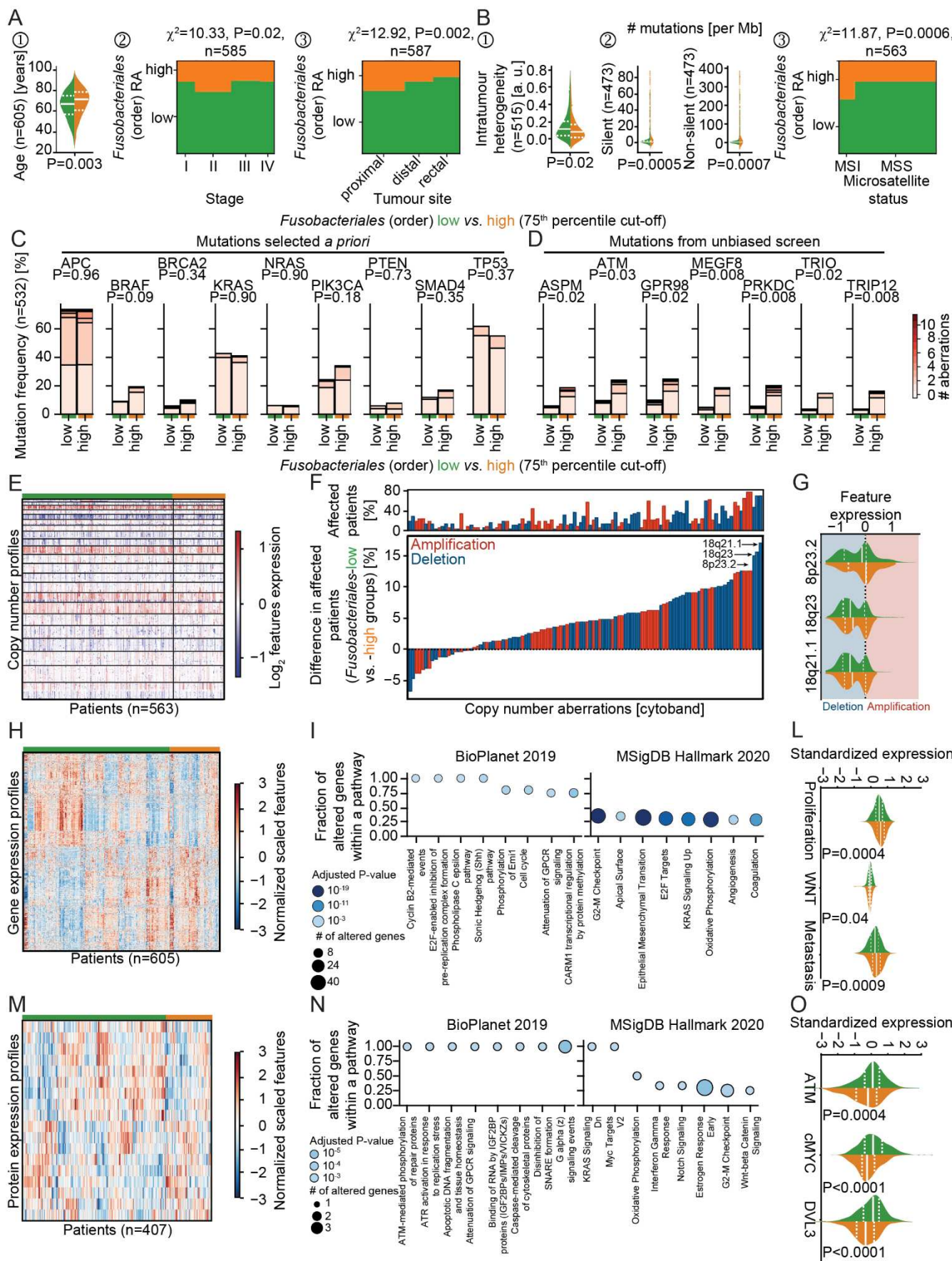
428 **B-D.** Per-patient (waterfall plot, **1**, left) and distribution (violin plot with overlaid data-points, **2**, right)
429 of bacterium prevalence in tumour resections of the Taxonomy (n=140, **B**) and TCGA-COAD-READ
430 (n=605, **D**). In **B-D 1**, patients are sorted in ascending order by prevalence of either *Fn* (Taxonomy
431 cohort, **B**) or *Fusobacteriales* at the order taxonomic rank (TCGA-COAD-READ cohort, **D**). Cut-off of
432 75th percentile used for patients' stratification in downstream analysis is also indicated (black dotted
433 line). Corresponding per-patient fraction of *Fn* species to total *Fusobacteriales* order relative
434 abundance detected for the TCGA-COAD-READ cohort is shown in **C**.

435 **E-F.** Violin plots grouped by prevalence of either *Fn* (Taxonomy cohort, **E**) or *Fusobacteriales* at the
436 order taxonomic rank (TCGA-COAD-READ cohort, **F**) depicting the expression distribution of key
437 genes or signatures involved in inflammation and immuno-suppression. Median and lower (25th) and
438 upper (75th) percentiles are indicated by white solid or dashed lines, respectively.

439 **G-H.** Stacked bar plots indicating cell type composition per-patient estimated from gene expression by
440 quanTIseq in tumours with low vs. high prevalence of either *Fn* (Taxonomy cohort, **G**) or
441 *Fusobacteriales* at the order taxonomic rank (TCGA-COAD-cohort, **H**). Cell type composition is
442 shown sorted in ascending order of tumour and stromal content (**1** and **3**) and aggregated (by mean, **2**
443 across the low- and high- subgroups).

444 **I.** Distribution of specific tumour/stroma and immune cell types determined as indicated by either
445 quanTIseq or MCPcounter grouped by either *Fn* (Taxonomy cohort) or *Fusobacteriales* at the order
446 taxonomic rank (TCGA-COAD-READ cohort). Median and lower (25th) and upper (75th) percentiles
447 are indicated by white solid or dashed lines, respectively.

Figure 3.



450 **Multi-omic characterization of the association between *Fusobacteriales* relative abundance and**
451 **human host tumour microenvironment in the TCGA-COAD-READ cohort.**

452 **A-B.** Association between *Fusobacteriales* at the order taxonomic rank binned into high vs. low (cut-
453 off 75th percentile) and clinico-pathological (**A**) and mutational (**B**) characteristics of the human host.

454 **C-D.** Comparison of frequency of occurrence of mutations selected *a priori* (**C**) or identified by an
455 unbiased scan (**D**) in *Fusobacteriales*-high vs -low patients. Colorbar indicates number of detected
456 aberrations among frame shift deletions and insertions, in frame deletions and insertions, missense and
457 nonsense mutations and splice sites. P-values were computed with χ^2 independence tests and adjusted
458 for multiple comparisons (Benjamini-Hochberg false discovery rate).

459 **E-G.** Heatmap (**E**) displaying copy number alterations grouped by *Fusobacteriales*-high (in orange)
460 and -low (in green) relative abundance. Waterfall plot (**F**) displaying differences in recurrent copy
461 number aberrations detected in patients with low- vs. high *Fusobacteriales*. Top panel in **F** reports
462 percentage of patients affected by recurrent copy number aberrations. Distribution of top 3 deletions
463 whose frequency of occurrence differs between *Fusobacteriales*-high and -low patients (**G**). Red and
464 blue shading indicates amplification and deletions, respectively.

465 **H-L.** Heatmap (**H**) displaying expression of genes differentially expressed when comparing
466 *Fusobacteriales*-high vs. low patients and corresponding pathway enrichment analysis (**I**). Expression
467 distribution grouped by *Fusobacteriales* RA for selected gene expression signatures is shown in **L**.

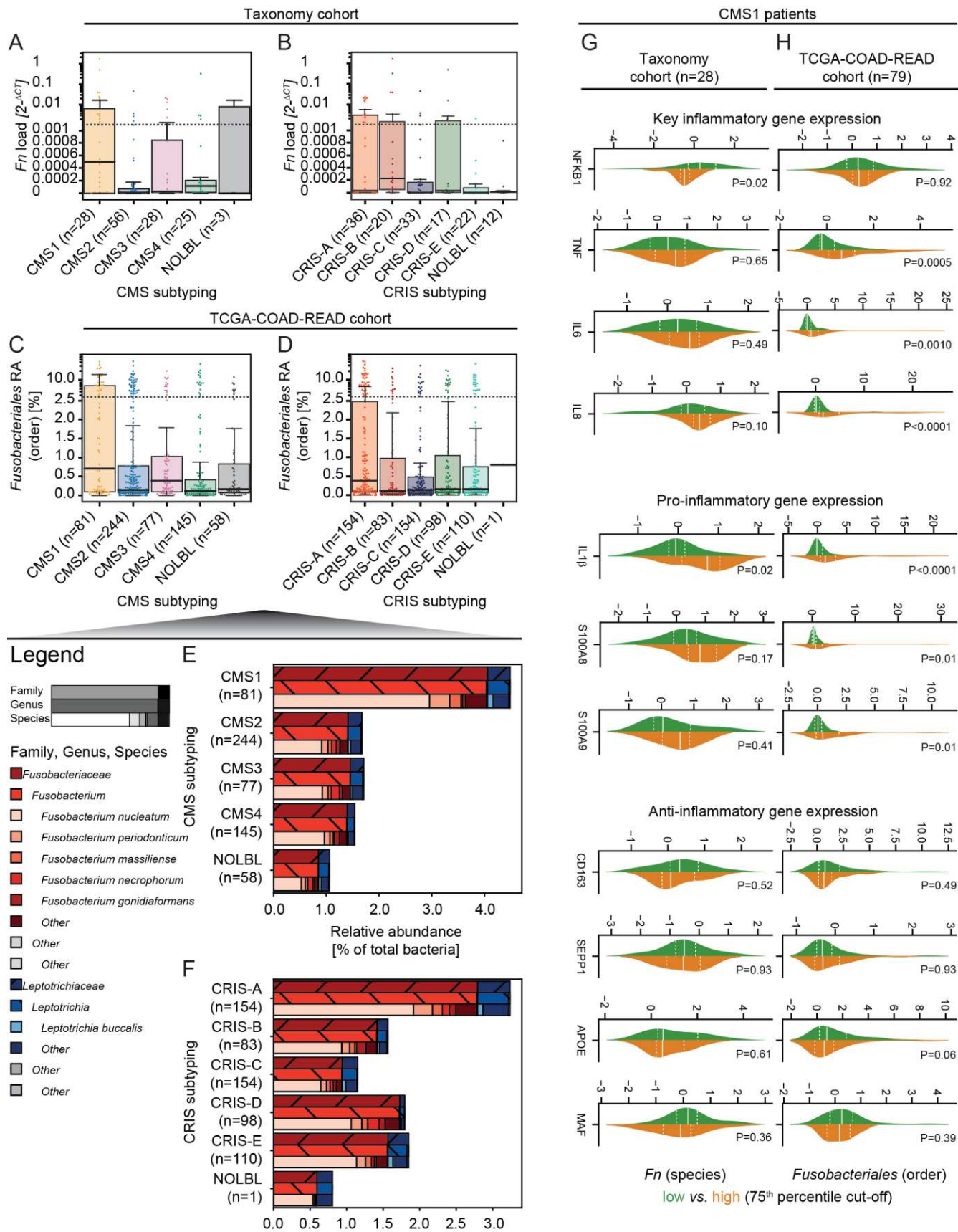
468 **M-O.** Heatmap (**M**) displaying expression of proteins differentially expressed when comparing
469 *Fusobacteriales*-high vs. low patients and corresponding pathway enrichment analysis (**N**). Expression
470 distribution grouped by *Fusobacteriales* RA for key proteins is shown in **O**.

471 In violin plots, the median and lower (25th) and upper (75th) percentiles are indicated by white solid or
472 dashed lines, respectively.

473 Orange and green annotation bars denote patients with high vs. low *Fusobacteriales* relative abundance
474 (75th percentile cut-off).

475 (Unadjusted) P-values in **L** and **O** were determined by Kruskal-Wallis H-test for independent samples.

Figure 4.



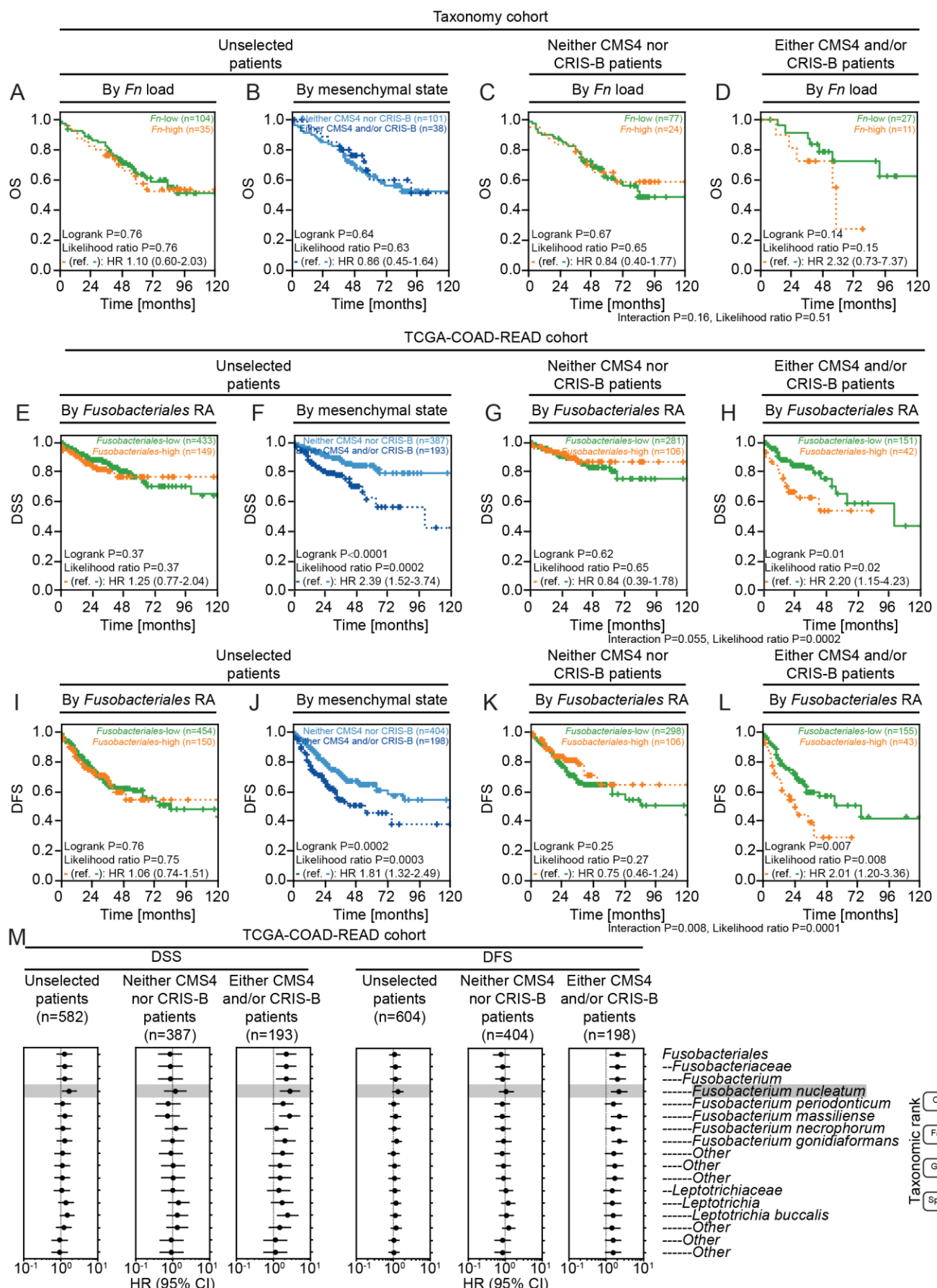
478 **Prevalence of *Fn*/Fusobacteriales by transcriptomic-based molecular subtypes of the host.**

479 **A-D.** Boxplot with overlaid dot plots displaying the dependency by CMS (**A, C**) and CRIS (**B, D**)
480 molecular subtyping by prevalence of either *Fn* (Taxonomy cohort, **A-B**) or *Fusobacteriales* at the
481 order taxonomic rank (TCGA-COAD-READ cohort, **C-D**).

482 **E-F.** Relative abundance (to total bacterial kingdom) of *Fusobacteriales* reported at increasing
483 resolution of taxonomic rank (family, genus and species) by CMS (**E**) and CRIS (**F**) subtypes
484 (aggregated by mean).

485 **G-H** Distribution of key (pro-)/(anti-)inflammatory genes grouped by either *Fn* (Taxonomy cohort, **G**)
486 or *Fusobacteriales* at the order taxonomic rank (TCGA-COAD-READ cohort, **H**) restricted to CMS1
487 patients. Median and lower (25th) and upper (75th) percentiles are indicated by white solid or dashed
488 lines, respectively. (Unadjusted) P-values were determined by Kruskal-Wallis H-test for independent
489 samples.

Figure 5.



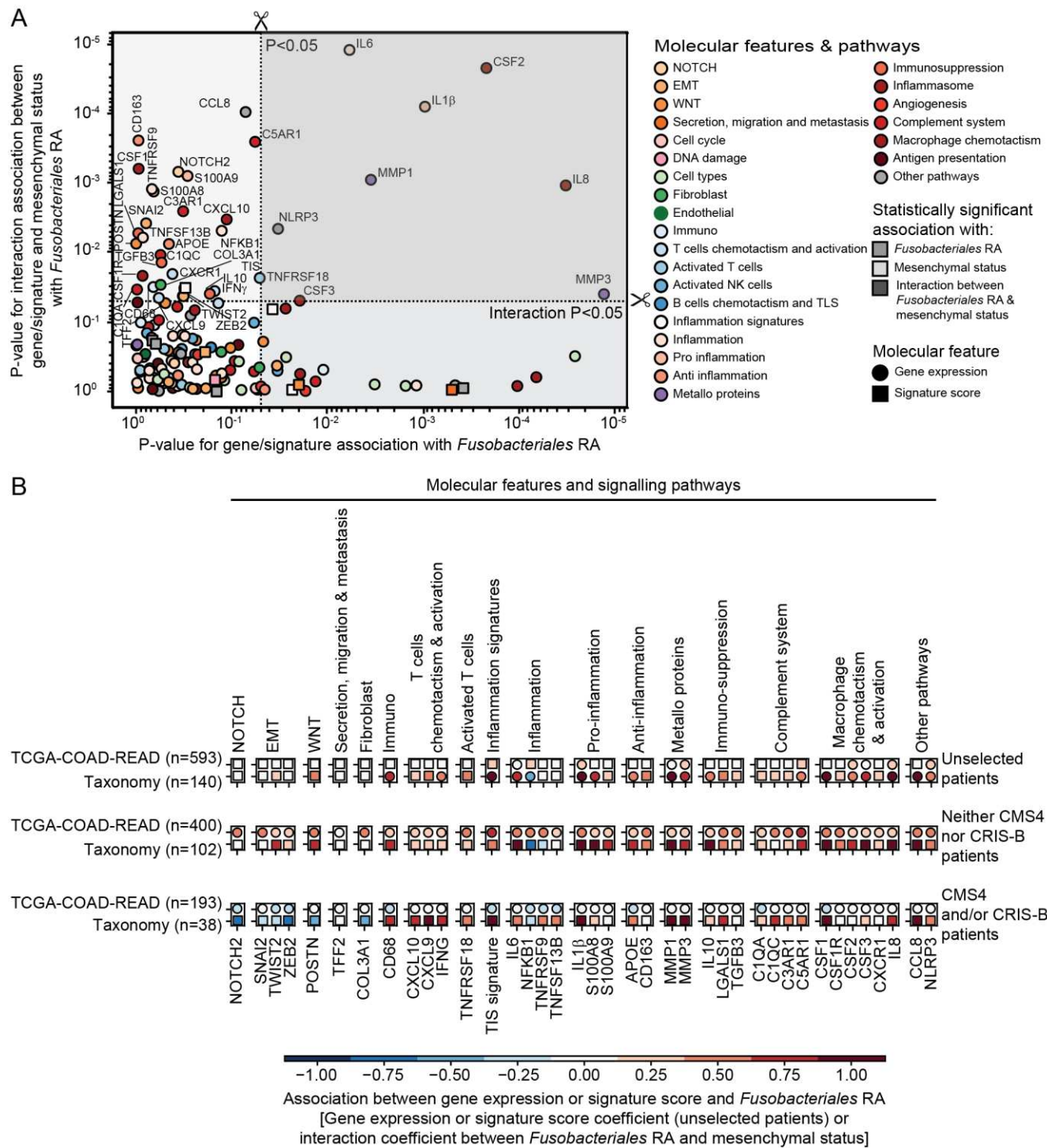
492 **High *Fn*/Fusobacteriales prevalence is associated with negative clinical outcome in patients with**
493 **mesenchymal-like tumours.**

494 **A-L.** Kaplan-Meier estimates comparing survival curves in patients of the Taxonomy (OS, **A-D**) and
495 TCGA-COAD-READ (DSS and DFS, **E-L**) cohorts. Patients across the whole cohort were grouped by
496 prevalence (high vs. low based on 75th percentile cut-off) in **A, E, I** or mesenchymal status (CMS4
497 and/or CRIS-B vs. remaining cases) in **B, F, J**. Patients were grouped by prevalence and further
498 stratified by mesenchymal status in **C-D, G-H, K-L**. Prevalence refers to either *Fn* load or
499 *Fusobacteriales* RA at the order level for the Taxonomy and TCGA-COAD-READ cohorts,
500 respectively.

501 **M.** Cox regression models fitted on bacterium RA reported at the order, family, genus and species
502 taxonomic ranks. For each taxonomic rank, patients were classified as low or high prevalence using the
503 corresponding 75th percentile RA abundance as cut-off. Univariate Cox regression models were fitted
504 when evaluating association between pathogen prevalence (high vs. low; reference low) at each
505 taxonomic rank and either DSS or DFS in the whole unselected patient population (left panel). Cox
506 regression models with an interaction term between pathogen prevalence (high vs. low; reference low)
507 and mesenchymal status (mesenchymal, i.e. either CMS4 and/or CRIS-B, vs. non-mesenchymal, i. e.
508 neither CMS4 nor CRIS-B) at each taxonomic rank and either DSS or DFS were fitted to evaluate
509 differential impact of bacterium on clinical outcome by tumour biology (right panels).

510

Figure 6.



511

512 *Exploration of mechanism underlying differential impact of Fusobacteriales in mesenchymal*
513 *vs. non-mesenchymal tumours.*

514 **A.** Scatterplot depicting P-values derived by assessing with logistic regression models the relationship
515 between genes/signatures associated with *Fusobacteriales* RA in univariate analysis (model 1, x axis)
516 or the interaction with mesenchymal status (model 2, y axis).
517 **B.** Breakdown of association including direction, effect size, in the unselected patients' population and
518 within mesenchymal vs. non-mesenchymal cases. Only gene/signatures with significant interaction
519 between *Fusobacteriales* RA and the gene/signature interaction with the molecular subtype (model 2)
520 in the TCGA-COAD-READ cohort are included. Associations for both the TCGA-COAD-READ
521 (*Fusobacteriales* RA) and Taxonomy (*Fn* load) cohorts are shown. Statistically significant associations
522 are represented with circle markers whereas non-significant associations are indicated by squared
523 markers.

524 **References**

525 1 Bray F, Ferlay J, Soerjomataram I *et al.* Global cancer statistics 2018: GLOBOCAN estimates of
526 incidence and mortality worldwide for 36 cancers in 185 countries. *CA: A Cancer Journal for*
527 *Clinicians* 2018;68:394–424. doi:10.3322/caac.21492

528 2 Guinney J, Dienstmann R, Wang X *et al.* The consensus molecular subtypes of colorectal cancer.
529 *Nature Medicine* 2015;21:1350–6. doi:10.1038/nm.3967

530 3 Isella C, Brundu F, Bellomo SE *et al.* Selective analysis of cancer-cell intrinsic transcriptional traits
531 defines novel clinically relevant subtypes of colorectal cancer. *Nature Communications* 2017;8:15107.
532 doi:10.1038/ncomms15107

533 4 Routy B, Gopalakrishnan V, Daillère R *et al.* The gut microbiota influences anticancer
534 immunosurveillance and general health. *Nature Reviews Clinical Oncology* 2018;15:382–96.
535 doi:10.1038/s41571-018-0006-2

536 5 Flanagan L EM Schmid J. *Fusobacterium nucleatum* associates with stages of colorectal neoplasia
537 development, colorectal cancer and disease outcome. *Eur J Clin Microbiol Infect Dis* Published Online
538 First: 2014. doi:10.1007/s10096-014-2081-3

539 6 McCoy AN, Araújo-Pérez F, Azcárate-Peril A *et al.* *Fusobacterium* is associated with colorectal
540 adenomas. *PLoS ONE* 2013;8:e53653. doi:10.1371/journal.pone.0053653

541 7 Kostic AD, Gevers D, Pedamallu CS *et al.* Genomic analysis identifies association of *fusobacterium*
542 with colorectal carcinoma. *Genome Research* 2012;22:292–8. doi:10.1101/gr.126573.111

543 8 Kostic AD, Chun E, Robertson L *et al.* *Fusobacterium nucleatum* Potentiates Intestinal
544 Tumorigenesis and Modulates the Tumor-Immune Microenvironment. *Cell Host and Microbe*
545 2013;14:207–15. doi:10.1016/j.chom.2013.07.007

546 9 Ito M, Kanno S, Noshio K *et al.* Association of *Fusobacterium nucleatum* with clinical and molecular
547 features in colorectal serrated pathway. *International Journal of Cancer* 2015;137:1258–68.
548 doi:10.1002/ijc.29488

549 10 Bullman S, Pedamallu CS, Sicinska E *et al.* Analysis of *Fusobacterium* persistence and antibiotic
550 response in colorectal cancer. *Science* 2017;358:1443–8. doi:10.1126/science.aal5240

551 11 Kinross J, Mirnezami R, Alexander J *et al.* A prospective analysis of mucosal microbiome-
552 metabonome interactions in colorectal cancer using a combined MAS 1H NMR and metataxonomic
553 strategy. *Scientific Reports* 2017;7:8979. doi:10.1038/s41598-017-08150-3

554 12 Brennan CA, Garrett WS. *Fusobacterium nucleatum* symbiont, opportunist and oncobacterium.
555 *Nature Reviews Microbiology* 2018;17:156–66. doi:10.1038/s41579-018-0129-6

556 13 Mima K, Sukawa Y, Nishihara R *et al.* *Fusobacterium nucleatum* and T cells in colorectal
557 carcinoma. *JAMA Oncology* 2015;1:653–61. doi:10.1001/jamaoncol.2015.1377

558 14 Lee D-W, Han S-W, Kang J-K *et al.* Association between *fusobacterium nucleatum*, pathway
559 mutation, and patient prognosis in colorectal cancer. *Annals of Surgical Oncology* 2018;25:3389–95.
560 doi:10.1245/s10434-018-6681-5

561 15 Kunzmann AT, Proença MA, Jordao HW *et al.* *Fusobacterium nucleatum* tumor DNA levels are
562 associated with survival in colorectal cancer patients. *European Journal of Clinical Microbiology &*

563 *Infectious Diseases* 2019;38:1891–9. doi:10.1007/s10096-019-03649-1

564 16 Gethings-Behncke C, Coleman HG, Jordao HW *et al.* *Fusobacterium nucleatum* in the colorectum
565 and its association with cancer risk and survival: A systematic review and meta-analysis. *Cancer*
566 *Epidemiology Biomarkers & Prevention* 2020;29:539–48. doi:10.1158/1055-9965.epi-18-1295

567 17 Castellarin M, Warren RL, Freeman JD *et al.* *Fusobacterium nucleatum* infection is prevalent in
568 human colorectal carcinoma. *Genome Research* 2012;22:299–306. doi:10.1101/gr.126516.111

569 18 Dharmani P, Strauss J, Ambrose C *et al.* *Fusobacterium nucleatum* infection of colonic cells
570 stimulates MUC2 mucin and tumor necrosis factor alpha. *Infection and Immunity* 2011;79:2597–607.
571 doi:10.1128/IAI.05118-11

572 19 Allen WL, Dunne PD, McDade S *et al.* Transcriptional Subtyping and CD8 Immunohistochemistry
573 Identifies Patients With Stage II and III Colorectal Cancer With Poor Prognosis Who Benefit From
574 Adjuvant Chemotherapy. *JCO Precision Oncology* 2018;44:1–15. doi:10.1200/po.17.00241

575 20 McCorry AM, Loughrey MB, Longley DB *et al.* Epithelial-to-mesenchymal transition signature
576 assessment in colorectal cancer quantifies tumour stromal content rather than true transition. *Journal of*
577 *Pathology* 2018;**246**:422–6. doi:10.1002/path.5155

578 21 Biosciences M. Nbt.1868.Pdf. *Nature Publishing Group* 2011;**29**. doi:10.1038/nbt0511-393

579 22 Walker MA, Pedamallu CS, Ojesina AI *et al.* GATK PathSeq: a customizable computational tool
580 for the discovery and identification of microbial sequences in libraries from eukaryotic hosts.
581 *Bioinformatics (Oxford, England)* 2018;**34**:4287–9. doi:10.1093/bioinformatics/bty501

582 23 Finotello F, Mayer C, Plattner C *et al.* Molecular and pharmacological modulators of the tumor
583 immune contexture revealed by deconvolution of RNA-seq data. *Genome Medicine* 2019;**11**.
584 doi:10.1186/s13073-019-0638-6

585 24 Becht E, Giraldo NA, Lacroix L *et al.* Estimating the population abundance of tissue-infiltrating
586 immune and stromal cell populations using gene expression. *Genome Biology* 2016;**17**:218.
587 doi:10.1186/s13059-016-1070-5

588 25 Carvalho AC de, Mattos Pereira L de, Datorre JG *et al.* Microbiota profile and impact of
589 fusobacterium nucleatum in colorectal cancer patients of barretos cancer hospital. *Frontiers in*
590 *Oncology* 2019;**9**. doi:10.3389/fonc.2019.00813

591 26 Mermel CH, Schumacher SE, Hill B *et al.* GISTIC2.0 facilitates sensitive and confident localization
592 of the targets of focal somatic copy-number alteration in human cancers. *Genome Biology* 2011;**12**.
593 doi:10.1186/gb-2011-12-4-r41

594 27 Serna G, Ruiz-Pace F, Hernando J *et al.* Fusobacterium nucleatum persistence and risk of recurrence
595 after preoperative treatment in locally advanced rectal cancer. *Annals of Oncology* 2020;**xxx**.
596 doi:10.1016/j.annonc.2020.06.003

597 28 Purcell RV, Visnovska M, Biggs PJ *et al.* Distinct gut microbiome patterns associate with consensus
598 molecular subtypes of colorectal cancer. *Scientific Reports* 2017;**7**. doi:10.1038/s41598-017-11237-6

599 29 Ji S, Shin JE, Kim YC *et al.* Intracellular degradation of fusobacterium nucleatum in human
600 gingival epithelial cells. *Molecules and Cells* 2010;**30**:519–26. doi:10.1007/s10059-010-0142-8

601 30 Umaña A, Sanders BE, Yoo CC *et al.* Utilizing whole fusobacterium genomes to identify, correct,
602 and characterize potential virulence protein families. *Journal of Bacteriology* 2019;**201**.
603 doi:10.1128/jb.00273-19

604 31 Hamarsheh S, Zeiser R. NLRP3 inflammasome activation in cancer: A double-edged sword.
605 *Frontiers in Immunology* 2020;**11**. doi:10.3389/fimmu.2020.01444

606 32 Dinarello CA, Simon A, Meer JWM van der. Treating inflammation by blocking interleukin-1 in a
607 broad spectrum of diseases. *Nature Reviews Drug Discovery* 2012;**11**:633–52. doi:10.1038/nrd3800

608 33 Ortiz P, Bissada N, Palomo L *et al.* Periodontal therapy reduces the severity of active rheumatoid
609 arthritis in patients treated with or without tumor necrosis factor inhibitors. *Journal of Periodontology*
610 2009;**80**:535–40. doi:10.1902/jop.2009.080447

611 34 Choy EH, Benedetti FD, Takeuchi T *et al.* Translating IL-6 biology into effective treatments.
612 *Nature Reviews Rheumatology* 2020;**16**:335–45. doi:10.1038/s41584-020-0419-z

613 35 Parhi L, Alon-Maimon T, Sol A *et al.* Breast cancer colonization by *Fusobacterium nucleatum*
614 accelerates tumor growth and metastatic progression. *Nature Communications* 2020;**11**:1–12.
615 doi:10.1038/s41467-020-16967-2

616 36 Erez N, Truitt M, Olson P *et al.* Cancer-associated fibroblasts are activated in incipient neoplasia to
617 orchestrate tumor-promoting inflammation in an nf-kappaB-dependent manner. *Cancer Cell*
618 2010;**17**:135–47. doi:10.1016/j.ccr.2009.12.041

619 37 Shah K, Ahmed M, Kazi JU. The aurora kinase beta-catenin axis contributes to dexamethasone
620 resistance in leukemia. *npj Precision Oncology* 2021;**5**. doi:10.1038/s41698-021-00148-5

621 38 Pitts TM, Bradshaw-Pierce EL, Bagby SM *et al.* Antitumor activity of the aurora a selective kinase
622 inhibitor, alisertib, against preclinical models of colorectal cancer. *Oncotarget* 2016;**7**:50290–301.
623 doi:10.18632/oncotarget.10366

624 39 Brockmann M, Poon E, Berry T *et al.* Small molecule inhibitors of aurora-a induce proteasomal
625 degradation of n-myc in childhood neuroblastoma. *Cancer Cell* 2013;**24**:75–89.
626 doi:10.1016/j.ccr.2013.05.005

627 40 Stemmler MP, Eccles RL, Brabertz S *et al.* Non-redundant functions of EMT transcription factors.
628 *Nature Cell Biology* 2019;21:102–12. doi:10.1038/s41556-018-0196-y

629 41 Cox TR. The matrix in cancer. *Nature Reviews Cancer* Published Online First: February 2021.
630 doi:10.1038/s41568-020-00329-7

631 42 Desch A, Strozyk EA, Bauer AT *et al.* Highly invasive melanoma cells activate the vascular
632 endothelium via an MMP-2/integrin alpha beta induced secretion of vegf-a. *The American Journal of*
633 *Pathology* 2012;181:693–705. doi:10.1016/j.ajpath.2012.04.012

634 43 LEE KY, KIM Y-J, YOO H *et al.* Human brain endothelial cell-derived cox-2 facilitates
635 extravasation of breast cancer cells across the bloodbrain barrier. *Anticancer Research* 2011;31:4307–
636 13.https://ar.iiarjournals.org/content/31/12/4307

637 44 Winer A, Adams S, Mignatti P. Matrix metalloproteinase inhibitors in cancer therapy: Turning past
638 failures into future successes. *Molecular Cancer Therapeutics* 2018;17:1147–55. doi:10.1158/1535-
639 7163.mct-17-0646

640 45 Bendell JC, Starodub A, Huang X *et al.* A phase 3 randomized, double-blind, placebo-controlled
641 study to evaluate the efficacy and safety of GS-5745 combined with mFOLFOX6 as first-line treatment
642 in patients with advanced gastric or gastroesophageal junction adenocarcinoma. *Journal of Clinical*
643 *Oncology* 2017;35:TPS4139–9. doi:10.1200/jco.2017.35.15_suppl.tps4139

644 46 Mehta RS, Nishihara R, Cao Y *et al.* Association of dietary patterns with risk of colorectal cancer
645 subtypes classified by fusobacterium nucleatum in tumor tissue. *JAMA Oncology* 2017;3:921.
646 doi:10.1001/jamaoncol.2016.6374

647 47 Green D, Eyre H, Singh A *et al.* Targeting the MAPK7/MMP9 axis for metastasis in primary bone
648 cancer. *Oncogene* 2020;39:5553–69. doi:10.1038/s41388-020-1379-0

649 48 Ligorio M, Sil S, Malagon-Lopez J *et al.* Stromal microenvironment shapes the intratumoral
650 architecture of pancreatic cancer. *Cell* 2019;178:160–175.e27. doi:10.1016/j.cell.2019.05.012

651 49 Strosberg JR, Yeatman T, Weber J *et al.* A phase II study of RO4929097 in metastatic colorectal
652 cancer. *European Journal of Cancer* 2012;48:997–1003. doi:10.1016/j.ejca.2012.02.056

653 50 Lang J, Zhao X, Qi Y *et al.* Reshaping prostate tumor microenvironment to suppress metastasis via
654 cancer-associated fibroblast inactivation with peptide-assembly-based nanosystem. *ACS Nano*
655 2019;13:12357–71. doi:10.1021/acsnano.9b04857

656 51 Tauriello DVF, Palomo-Ponce S, Stork D *et al.* TGF-beta drives immune evasion in genetically
657 reconstituted colon cancer metastasis. *Nature* 2018;554:538–43. doi:10.1038/nature25492

658 52 Freedman JD, Duffy MR, Lei-Rossmann J *et al.* An oncolytic virus expressing a t-cell engager
659 simultaneously targets cancer and immunosuppressive stromal cells. *Cancer Research* 2018;78:6852–
660 65. doi:10.1158/0008-5472.can-18-1750

661 53 Ping Q, Yan R, Cheng X *et al.* Cancer-associated fibroblasts: Overview, progress, challenges, and
662 directions. *Cancer Gene Therapy* Published Online First: March 2021. doi:10.1038/s41417-021-00318-
663 4

664 54 Casasanta MA, Yoo CC, Udayasuryan B *et al.* Fusobacterium nucleatum host-cell binding and
665 invasion induces IL-8 and CXCL1 secretion that drives colorectal cancer cell migration. *Science
666 Signaling* 2020;13. doi:10.1126/SCISIGNAL.ABA9157